

Spin-singlet dimer phase in a frustrated square lattice under a magnetic field

L. M. Ramos^a, M. Schmidt^b, F. M. Zimmer^a

^a*Instituto de Física - Universidade Federal de Mato Grosso do Sul, Campo Grande, 79070-900, MS, Brazil*

^b*Departamento de Física - Universidade Federal de Santa Maria, Santa Maria, 97105-900, RS, Brazil*

Abstract

We investigated the isotropic spin- $\frac{1}{2}$ Heisenberg model on an anisotropic square lattice with competing exchange interactions, motivated by the unconventional magnetic behavior observed in the verdazyl-based compound (*o*-MePy-V)PF₆. Using a cluster mean-field approach, we explore a field-induced phase stabilized by the interplay between frustration and quantum fluctuations, focusing on the role of exchange interactions. We identify: (i) the formation of spin singlet pairs, signaled by enhanced spin–spin correlations in specific field regimes; and (ii) a one-half magnetization plateau, emerging from a subtle balance between competing exchange couplings and field-enhanced quantum fluctuations. Our results reveal that an enhancement of frustration, achieved by tuning small variations in the spatially anisotropic exchange interactions of the compound (*o*-MePy-V)PF₆, can stabilize a field-induced quantum phase where ferromagnetism coexists with antiferromagnetic dimers. Our results provide microscopic insight into the mechanisms driving these nontrivial phases and offer theoretical support for interpreting experimental observations in this class of low-dimensional quantum magnets.

Keywords: magnetic frustration, frustrated spin systems, quantum fluctuations, field-induced quantum phases, cluster mean-field theory

1. Introduction

Magnetic systems have long served as fertile ground for uncovering emergent quantum phenomena, especially when competing interactions create a rich landscape of degenerate ground states and excitations [1, 2]. For instance, the combination of competing interactions, low dimensionality and strong quantum fluctuations can stabilize a variety of unconventional phases such as spin liquids [3, 4, 5], valence bond solids [6], and fractional magnetization plateaus [7]. These states of matter are not only of fundamental interest but also provide insights into entanglement [8, 9], quantum criticality [10], and exotic excitations such as spinons [11, 12] and triplons [13, 14]. Moreover, tuning quantum fluctuations via an external magnetic field in frustrated systems can lead to intriguing effects [15, 16], such as the coexistence of magnetization plateaus and dimerized states [17]. An important question concerns whether the degree of frustration can play a central role

in the stability of such states. In the present work, we investigate this issue on a spin-1/2 frustrated square lattice with anisotropic interactions that hosts a spin-singlet state.

Frustration can arise in a variety of systems, either from the lattice geometry or due to the nature and range of the interactions. Typical candidates for exhibiting frustration include triangular-based lattices with anti-ferromagnetic (AF) exchange interactions [18, 19], disordered systems such as spin glasses [20, 21, 22, 23], and even bipartite lattices when there is competition between nearest- and next-nearest-neighbor interactions or between AF and ferromagnetic (FM) couplings [24, 5]. In particular, the presence of FM and AF couplings on different bonds can introduce a subtle competition, in which a delicate balance of interactions can favor ground states with nontrivial spin arrangements in bipartite systems [25]. A prototypical example is found in spin-ladder systems, where AF interchain (rung) interactions compete with FM intrachain (leg) couplings, giving rise to a rich variety of unconventional magnetic phases, including partially ordered states, spin-singlet dimer phases, and magnetization plateaus under applied magnetic fields [26, 27, 28, 29].

Email addresses: lucas.morais@ufms.br (L. M. Ramos), mateus.schmidt@ufrsm.br (M. Schmidt), fabio.zimmer@ufms.br (F. M. Zimmer)

Another interesting example of competitive system is found in the verdazyl-based molecular compound (*o*-MePy-V)PF₆, which provides a compelling platform for studying frustrated quantum magnetism [15]. This compound features a quasi-two-dimensional spin-1/2 square lattice, with PF₆ anions intercalated between the layers, and exhibits a collinear AF ground state with twofold periodicity at zero magnetic field. However, its magnetization under an applied magnetic field deviates from conventional behavior, exhibiting an increase with alternating concavity, featuring a plateau-like structure at low temperatures. This outcome is well described by an anisotropic-lattice Heisenberg model [15, 17]. Remarkably, when the model also includes a weak spin anisotropy, the plateau-like behavior can evolve into a well-defined magnetization plateau. More importantly, the interplay between frustration and field-induced quantum fluctuations brings out the coexistence of FM and dimerized chains in this plateau regime [17].

It has been found that spin anisotropy can help stabilize this exotic state, which is absent in the isotropic spin regime. However, it is still unclear whether this dimerized state can also be accessed in the isotropic limit of the model through small changes in the exchange interactions proposed in Ref. [15]. Therefore, a natural question is whether tuning the exchange interactions and, thereby, the degree of frustration in the spin-1/2 Heisenberg model can lead to a field-induced dimerized state on the square lattice inspired by the compound (*o*-MePy-V)PF₆.

In this work, we present a theoretical investigation of the spin-1/2 Heisenberg model on a square lattice with six distinct nearest-neighbor exchange interactions under an external magnetic field. Our study focuses on how the competing exchange interactions and applied magnetic field can contribute to stabilizing novel quantum phases, with particular emphasis on: (i) the singlet-pair correlations, quantified through spin-spin correlation functions, and (ii) the emergence of one-half magnetization plateau, arising from the subtle balance between the degree of frustration and enhanced quantum fluctuations. We investigate the ground-state properties of this frustrated model by employing the cluster mean-field (CMF) method. This approach improves the conventional mean-field theory by incorporating exact calculations of the short-range correlations within finite-size clusters, while treating intercluster couplings at the mean-field level. This method has demonstrated remarkable accuracy in capturing essential features of frustrated quantum magnets at low temperatures, including magnetization plateaus, nontrivial quantum phase transitions, and nonmagnetic states that

arise from the competition between exchange interactions and quantum fluctuations [30, 31, 32, 33, 34]. The CMF method enables the identification of quantum phases and field-induced phenomena [17], offering quantitative agreement with previous numerical studies based on the tensor network method [15] and focused on the model proposed for the compound (*o*-MePy-V)PF₆.

After introducing the model in more detail in the following Sec. 2, we present the CMF results for the ground state and the effects of thermal fluctuations in Sec. 3. Finally, Sec. 4 summarizes the paper and presents our conclusion.

2. Model and method

We consider the spin- $\frac{1}{2}$ Heisenberg model on an anisotropic square lattice with six distinct nearest-neighbor exchange couplings J_n ($n = 1, \dots, 6$). The Hamiltonian is given by

$$H = - \sum_{\langle i,j \rangle} J_n \mathbf{S}_i \cdot \mathbf{S}_j - h^z \sum_i S_i^z, \quad (1)$$

where \mathbf{S}_i denotes the spin- $\frac{1}{2}$ operators at site i , and J_n represents the anisotropic exchange couplings between neighboring sites i and j . The last term in Eq. 1 represents the applied magnetic field h^z , which acts along the S^z spin component. The parametrization of J_n follows a similar pattern of signs to that adopted in the model proposed in Ref. [15] and is schematically illustrated in Fig. 1.

The lattice structure can be viewed as composed of two coupled spin chains (see Fig. 1). Chain 1 (gray sites) is a FM chain governed by couplings J_1 and J_6 , while chain 2 (black sites) consists of a mixed AF-FM chain with AF $J_2 < 0$ and FM $J_5 > 0$ couplings. The two chains are connected via AF interactions J_3 and J_4 , forming an anisotropic and frustrated square lattice. Frustration arises in square plaquettes containing an odd number of AF bonds, characterized by loops for which the product of exchange couplings satisfies $\prod_n J_n < 0$. In particular, loops involving J_2 are frustrated.

To investigate this system, we employ the CMF method, in which the infinite lattice is partitioned into identical clusters of eight sites, $n_s = 8$, as illustrated by the shaded regions of Fig. 1. The intercluster interactions are decoupled according to

$$\mathbf{S}_i \cdot \mathbf{S}_j \approx \mathbf{S}_i \cdot \langle \mathbf{S}_j \rangle + \langle \mathbf{S}_i \rangle \cdot \mathbf{S}_j - \langle \mathbf{S}_i \rangle \cdot \langle \mathbf{S}_j \rangle, \quad (2)$$

where $\langle \mathbf{S}_i \rangle$ represents the local magnetization at site i . This decoupling leads to the effective single-cluster

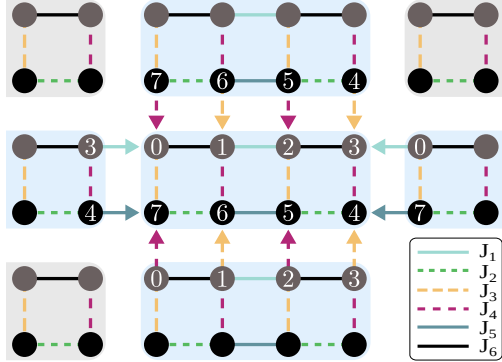


Figure 1: Schematic representation of the eight-site CMF approach applied to an anisotropic square lattice with six distinct exchange couplings J_n ($n = 1, \dots, 6$). Solid and dashed lines denote FM and AF exchange interactions, respectively. The gray sites form a FM chain connected by couplings J_1 and J_6 (referred to as chain 1), while the black sites form chain 2, composed of AF and FM couplings J_2 and J_5 . The two chains are coupled via AF interactions J_3 and J_4 , resulting in a frustrated square lattice geometry. Frustration arises in square plaquettes containing an odd number of AF bonds. Arrows indicate the bonds treated at the mean-field level within the CMF framework.

Hamiltonian

$$H_{\text{eff}} = - \sum_{\langle i,j \rangle} J_n \mathbf{S}_i \cdot \mathbf{S}_j - h^z \sum_i S_i^z - \sum_{\langle i,k \rangle} J_{\bar{n}} \sum_{\alpha} \left[S_i^{\alpha} \langle S_k^{\alpha} \rangle - \frac{1}{2} \langle S_i^{\alpha} \rangle \langle S_k^{\alpha} \rangle \right], \quad (3)$$

where $\langle i, k \rangle$ labels pairs of boundary sites in neighboring clusters coupled via $J_{\bar{n}}$, with $\langle S^{\alpha} \rangle$ denoting the local magnetization along the direction $\alpha = x, y, z$. In the present approach, we consider that the system exhibits identical patterns of local magnetizations across all clusters, which allows the local magnetizations of neighboring clusters $\langle S_k^{\alpha} \rangle$ to be obtained from the corresponding sites within the considered cluster. In this case, the summation $\sum_{\langle i,k \rangle}$ in Eq. (3) can be evaluated by replacing $\langle S_k^{\alpha} \rangle$ with the corresponding local magnetization pattern at the site of the considered cluster. For example, when $i = 0$, the sum term $J_{\bar{n}} S_i^{\alpha} \langle S_k^{\alpha} \rangle$ is replaced by $J_4 S_0^{\alpha} \langle S_7^{\alpha} \rangle + J_6 S_0^{\alpha} \langle S_3^{\alpha} \rangle$, where all the sites belong to the considered cluster.

The local magnetizations are determined self-consistently from the thermal expectation values

$$m_i^{\alpha} \equiv \langle S_i^{\alpha} \rangle = \frac{\text{Tr} (S_i^{\alpha} e^{-\beta H_{\text{eff}}})}{Z}, \quad Z = \text{Tr} (e^{-\beta H_{\text{eff}}}), \quad (4)$$

where $\beta = 1/(k_B T)$ and Z is the partition function of the cluster. In the zero-temperature limit, the expectation values reduce to the ground-state expectation values over the lowest-energy eigenstate.

The self-consistent solution corresponds to the stationary point that minimizes the variational free energy associated with the CMF ansatz. Specifically, the free energy per cluster is given by $F = -\frac{1}{\beta} \ln Z$. The physically stable solution corresponds to the minima of F with respect to the set of local magnetizations $\{m_i^{\alpha}\}$. This guarantees thermodynamic consistency within the CMF approximation.

Once the self-consistent solution is obtained, other thermodynamic quantities can be computed. The total magnetization is evaluated as

$$M = \sqrt{(M^x)^2 + (M^y)^2 + (M^z)^2}, \quad M^{\alpha} = \frac{1}{n_s} \sum_j m_j^{\alpha}, \quad (5)$$

and in order to characterize the magnetic properties of each chain individually, we define the average local moments

$$m_{c1}^2 = \frac{1}{4} \sum_{j=0}^3 \sum_{\alpha} \langle S_j^{\alpha} \rangle^2, \quad m_{c2}^2 = \frac{1}{4} \sum_{j=4}^7 \sum_{\alpha} \langle S_j^{\alpha} \rangle^2, \quad (6)$$

where sites $j = 0$ to 3 belong to chain 1 and sites $j = 4$ to 7 belong to chain 2. These quantities measure the average magnitude of the local spins within each chain, rather than their alignment (i.e., the sign of the local magnetizations is irrelevant for these quantities). Furthermore, the spin–spin correlation functions are calculated to probe the nature of quantum correlations and the presence of short-range order:

$$C_{ij} = \langle \mathbf{S}_i \cdot \mathbf{S}_j \rangle. \quad (7)$$

This procedure indicates that the CMF method provides a versatile framework for investigating various physical quantities, with intracluster dynamics fully accounted by exactly incorporating the interactions within each cluster. The intercluster interactions are treated self-consistently to capture local features of the model. In this sense, the CMF approach offers valuable insights into the interplay between quantum fluctuations, frustration, and external magnetic fields, particularly with regard to intracluster interactions. In the following section, the numerical results for the model investigated within the CMF framework are presented and analyzed.

3. Results and discussion

The set of local magnetizations (see Eq. (4)) is solved self-consistently for a cluster of up to 8 sites represented by Eq. (3), which is exactly diagonalized. For numerical purposes, we use the exchange interaction J_1 as the

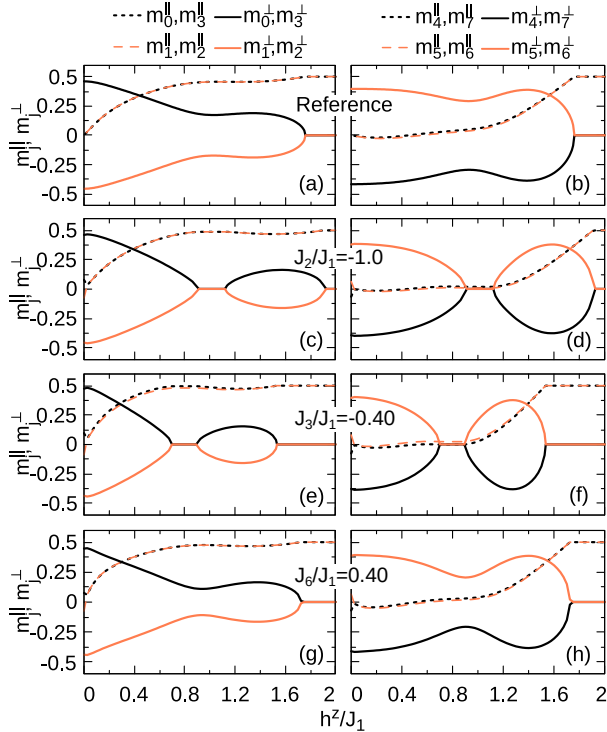


Figure 2: Longitudinal (dashed lines) and transverse (solid lines) components of the eight local magnetizations in the ground state under an external magnetic field for: (a) and (b) Reference system , (c) and (d) $J_2/J_1 = -1.0$, (e) and (f) $J_3/J_1 = -0.40$, (g) and (h) $J_6/J_1 = 0.40$. The left column displays the local moments of chain 1, while the right column shows the local moments of chain 2.

energy unit, setting the Boltzmann constant $k_B = 1$. We start from the exchange couplings reported for the compound (o-MePy-V)PF₆, given by $J_2/J_1 = -0.82$, $J_3/J_1 = -0.66$, $J_4/J_1 = -0.61$, $J_5/J_1 = 0.26$, and $J_6/J_1 = 0.20$ [15], and make small variations in these in order to explore possible field-induced singlet states. It means that the magnetic properties of the model are analyzed for different sets of exchange interactions by evaluating the Eqs. (5), (6), and (7). We first investigate the ground-state properties and then present the effects of thermal fluctuations on the magnetic correlations of the system.

3.1. Properties of the ground state

The compound (o-MePy-V)PF₆ provides an interesting experimental perspective for studying the interplay of frustration and field-induced quantum fluctuations. It has a molecular structure composed of two quantum spin chains coupled via AF interactions. This system can be represented by an anisotropic square lattice model with six nearest-neighbor exchange interactions, in which one of the chains present both FM and

AF couplings. The degree of frustration in the present anisotropic square lattice model is directly associated with the strength of the exchange interactions. The role of frustration in the field-induced magnetic properties can be clarified by slight changes in the interactions. Figure 2 exhibits the local magnetization patterns for each chain with different sets of exchange interactions. This allows us to analyze the effects caused by the variation of a single exchange parameter compared to the reference compound (o-MePy-V)PF₆ shown in Fig. 2(a) and 2(b). In Figs. 2(a) and 2(b), the longitudinal components vanish, whereas the transverse components are finite and antisymmetric at a zero magnetic field. As the magnetic field increases, the transverse components of chain 1 (left panel) monotonically decrease and vanish at a critical field, while the longitudinal components smoothly grow towards saturation. In contrast, the longitudinal components of chain 2 (right panel) exhibit a slight and unexpected reduction at low fields, in agreement with Refs. [15, 17]. The local magnetization pattern reveals a collinear AF order within the transverse plane at zero field, characterized by a two-fold periodicity structure. The Zeeman coupling suppresses this AF collinear order as the field increases.

A small variation only in the exchange coupling J_2 (from $J_2/J_1 = -0.82$ to $J_2/J_1 = -1.00$) leads to a substantial modification of the local magnetization pattern at finite field, as illustrated in Figs. 2(c) and 2(d). The longitudinal components of chain 1 present a small value at zero field, increasing smoothly to full polarization as the magnetic field increases. This dependence is comparable to that of the reference system. In contrast, the transverse components exhibit quite distinct behavior under an applied field. In both chains, the transverse components still indicate a collinear AF state in the absence of a field but gradually decrease, vanishing within a narrow field range. In particular, chain 2 evolves to a nonmagnetic regime characterized by the absence of both transverse and longitudinal local magnetizations, while chain 1 simultaneously develops a FM ordering. Further increasing the field leads to a continuous reemergence of these transverse components before they disappear in the saturation field. An analogous result is obtained when exchange parameters of the original compound are used except for J_3 , which is slightly reduced from $J_3/J_1 = -0.66$ to $J_3/J_1 = -0.40$ in Figs. 2(e) and 2(f). However, changing only the exchange parameter J_6 (from $J_6/J_1 = 0.20$ to $J_6/J_1 = 0.40$) does not significantly affect the local magnetization pattern (see 2(g) and 2(h)), which essentially exhibits behavior analogous to that of the reference system. These results suggest that small variations in the exchange parame-

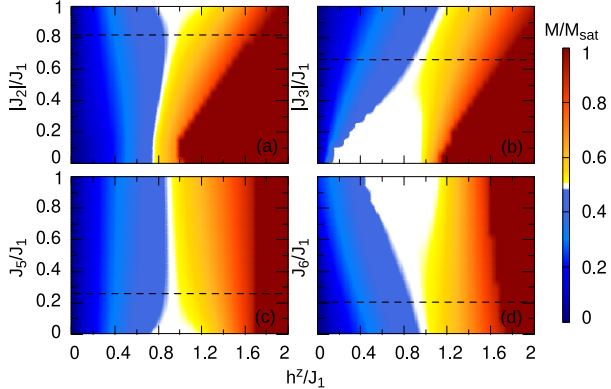


Figure 3: Normalized total magnetization as a function of the external magnetic field, with the exchange parameters of the compound (*o*-MePy-V)PF₆ kept fixed except for one, which is varied: (a) $|J_2|/J_1$, (b) $|J_3|/J_1$, (c) J_5/J_1 , and (d) J_6/J_1 . The dashed lines represent the reference values for the exchange interactions of the compound (*o*-MePy-V)PF₆. The one-half magnetization plateau is depicted as a broad white region in the diagram.

ter J_2 or J_3 can drive the system to a regime of strong quantum fluctuations induced by the field. In order to clarify this notable phenomenon, we will also investigate the behavior of magnetization plateaus, as well as the spin–spin correlation functions, under the effects of frustration arising from variations of such exchange parameters.

The role of these exchange parameters in the field-dependence of magnetization is depicted in the heat maps of Fig. 3. Each panel of this figure shows the effect of tuning a single exchange parameter away from the reference value [15], which is indicated by the dashed lines. As illustrated in Fig. 3(a), a one-half magnetization plateau (depicted as a broad white region in the diagram) appears when $|J_2|/J_1$ approaches J_1 in the range $0.9 \lesssim h^z/J_1 \lesssim 1.1$. On the other hand, reducing $|J_2|/J_1$ from the reference value suppresses this magnetization plateau and leads to saturation at lower magnetic field values. Notably, the occurrence of a well-defined magnetization plateau for higher AF J_2 couplings suggests an intriguing regime where a nontrivial phase can be obtained.

Enhancing the AF character of chain 2 proves crucial for stabilizing the one-half plateau state. This is supported by Fig. 3(c), where weakening the FM J_5 coupling in chain 2 expands the magnetization plateau region. However, our previous analysis is only valid when the chains are coupled by AF exchange interactions, which can lead to frustration. For example, Fig. 3(b) shows that the AF interaction J_3 directly affects the total magnetization of the ground state, with a one-

half plateau emerging for $|J_3|/J_1 \lesssim 0.5$. We also note that variations in J_4 yield analogous results due to their equivalence with J_3 in the lattice structure. As $|J_3|/J_1$ increases (or $|J_4|/J_1$), the AF character between chains becomes more pronounced, leading to a gradual suppression of the magnetization plateau. We propose that this affects the AF spin–spin correlation related to the interaction J_2 .

In summary, strengthening the AF character of the chain 2 enhances the degree of frustration in the square lattice, stabilizing the one-half plateau state in a regime dominated by quantum fluctuations induced by the field. As discussed in the following, the competition between frustration and field-induced quantum fluctuations can drive the emergence of nontrivial quantum phases within the plateau state. Similar mechanisms have been observed in other bipartite systems, where the interplay between frustration and quantum fluctuations leads to exotic dimerized phases [35]. Finally, as expected, enhancing the FM character of chain 1 can also be reflected in the rise in the one-half plateau state and the emergence of spontaneous magnetization at zero field (light blue color), as illustrated in Fig. 3(d). In particular, the results presented by Fig. 3 can help classify the choice of the reference system exchange parameters as belonging to a crossover region between the well-defined magnetization plateau and a plateau-like behavior. In summary, our results for the ground-state magnetization of this frustrated magnetic system are strongly dependent on the subtle balance between frustration and field-induced quantum fluctuations, revealing a rich phenomenology beyond the magnetism reported for the compound (*o*-MePy-V)PF₆ [15].

To account for the effects of external magnetic field on the plateau occurrence, we present in Fig. 4 the total magnetization and the average local moments of chains for some planes of the heat maps in Fig. 3 (corresponding to the same exchange parameters as set in Fig. 2). We begin by emphasizing that the total magnetization curve of the reference system, shown by the dashed lines in Fig. 4(a), exhibits a plateau-like behavior that closely resembles that obtained from tensor network calculations in Ref.[15]. Small variations in the exchange couplings relative to the reference system can either enhance this plateau-like feature or stabilize a well-defined magnetization plateau. Our findings support that increasing the AF J_2 interaction (relative to the reference system parameters) enhances the degree of frustration and amplifies the field-induced quantum fluctuations. This effect stabilizes the magnetization plateau state, as evidenced by the dark-blue curve in Fig. 4(a). In this case, the average magnetic moment of chain

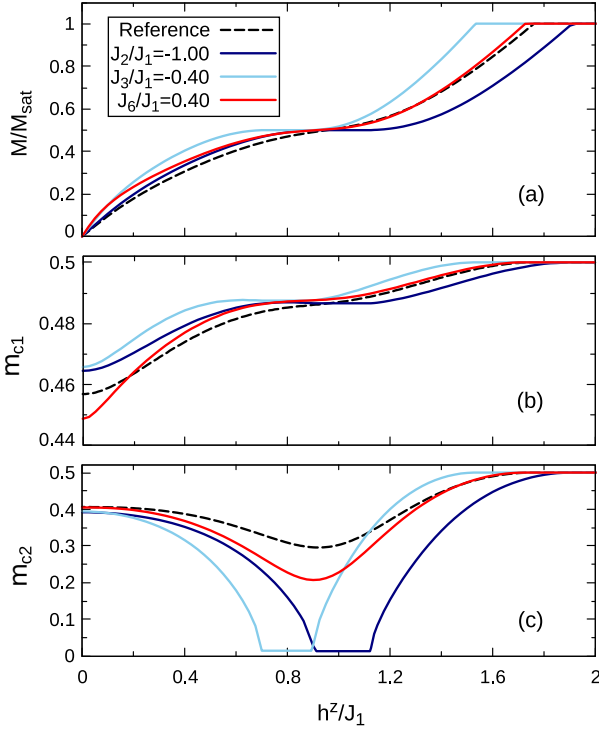


Figure 4: Ground state of the CMF model under magnetic field and different exchange interaction. (a) Total magnetization curve normalized by the saturation, (b) average local moments of chain 1 m_{c1} , and (c) average local moments of chain 2 m_{c2} . The dashed line indicates the exchange interactions of the reference compound (*o*-MePy-V)PF₆.

1 increases with field intensity but presents a constant value within the plateau range (see the dark-blue curve in Fig. 4(b)). In contrast, chain 2 undergoes a significant reduction in the average local moment due to the applied field. For $0.9 \lesssim h^z/J_1 \lesssim 1.1$, m_{c2} approaches zero (see the dark-blue curve in Fig. 4(c)), indicating that field-induced quantum fluctuations indeed destroy the local magnetic order. The presence of cusps in m_c reflects abrupt changes in the average magnitude of local moments within chain 2, such as enhanced spin fluctuations. Although the total magnetization M remains a smooth function of the magnetic field, spin-spin correlations of chain 2 can also signal this enhancement, as discussed in the following. These results show that the one-half plateau state for $J_2/J_1 = -1.0$ is characterized by full polarization in chain 1, while chain 2 realizes a nonmagnetic phase. Similar coexistence of polarized and nonmagnetic regions has been reported in other frustrated spin systems, including the field-induced plateau phase of Co₂V₂O₇, where inequivalent magnetic sites exhibit distinct behaviors under an applied field [7] as well as in spin-1/2 Heisenberg branched chains show-

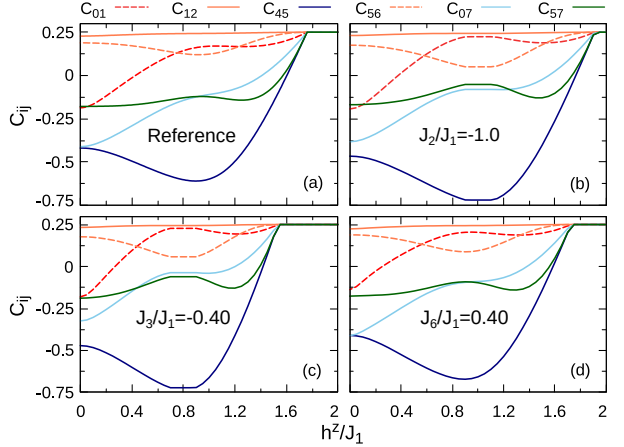


Figure 5: Field dependence of spin-spin correlation functions computed using eight-site CMF model at $T/J_1=0$ for (a) Reference compound, (b) $J_2/J_1 = -1.0$, (c) $J_3/J_1 = -0.40$ and (d) $J_6/J_1 = 0.40$. Some correlations have been omitted from the figure as they are nearly equivalent to those already shown, e.g., the correlations $C_{01} \approx C_{23}$, $C_{45} \approx C_{67}$, $C_{46} \approx C_{57}$ and the interchain correlations $C_{07} \approx C_{16} \approx C_{25} \approx C_{34}$.

ing ferrimagnetic plateaus stabilized by competing interactions [36]. Related phenomena also appear in coupled trimer chain models, where fractional magnetization plateaus emerge from the interplay of polarized and singlet states [37]. We emphasize that smooth behavior of magnetization near the plateau obtained in the present study contrasts with the findings for highly frustrated systems such as the kagome lattice [38], which exhibits cusps in the magnetization.

The coexistence of polarized states with the nonmagnetic phase can also be achieved by tuning other values of the exchange couplings. For instance, the light-blue curve in Fig. 4 illustrates this behavior for $J_3/J_1 = -0.40$ within the field range $0.7 \lesssim h^z/J_1 \lesssim 1.0$. In addition, an analogous result to that of the reference system is recovered by setting $J_6/J_1 = 0.40$ (see the red curve in Fig. 4), where chain 1 remains polarized along the field direction, while chain 2 exhibits a suppression of its average local moments.

The underlying physics of the previously discussed one-half magnetization plateau and nonmagnetic state in chain 2 can be further explored using spin-spin correlation functions. For example, Fig. 5(a) illustrates the field dependence of the C_{ij} for the reference system. At zero magnetic field, the C_{ij} values for chains 1 and 2 align with a collinear AF state, where C_{01} , C_{23} , C_{45} , and C_{67} show AF behavior, while C_{12} and C_{56} show FM correlations. As the magnetic field increases, the correlations C_{45} and C_{67} show an enhanced AF character, attributed to increased quantum fluctuations. This

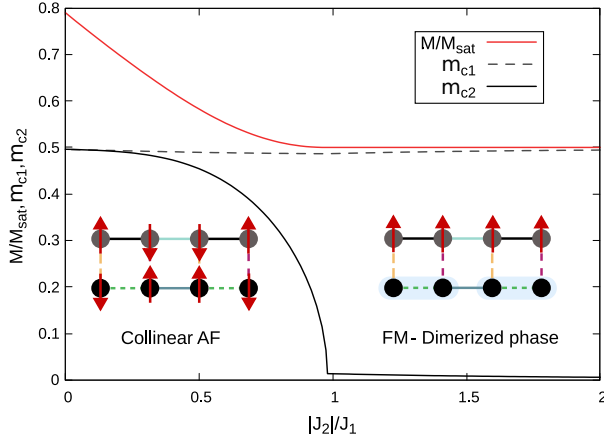


Figure 6: Total magnetization and average local moments of both quantum chains as a function of AF interaction $|J_2|/J_1$ at magnetic field $h^z/J_1 = 1.0$. The inset shows the FM-dimerized phases that arise for $|J_2|/J_1 > 1.0$.

increase in AF character is also observed when setting $J_2/J_1 = -1.0$ or $J_3/J_1 = -0.40$ (see Fig. 5(b) and 5(c)), but with a fundamental difference: the correlations C_{45} and C_{67} approach the perfect singlet value of -0.75 , while the interchain correlations (e.g., C_{07}, C_{16}, \dots) and C_{56} approach zero. Furthermore, the correlations C_{46} and C_{57} are also small, suggesting that chain 2 effectively forms singlet pairs and becomes dimerized due to the absence of local magnetic order (see Fig. 2(d) and 2(f)). This indicates that the one-half plateau state is effectively characterized by FM ordering in chain 1 and the realization of a spin-singlet dimer phase in chain 2. By changing only J_6 (from $J_6/J_1 = 0.20$ to $J_6/J_1 = 0.40$) in Fig. 5(d), the formation of singlet pairs described previously is absent, and the correlation pattern is similar to that of the reference compound.

Given the relevance of J_2 to the field-induced FM-dimerized phase, we present in Fig. 6 the dependence of the total magnetization and the average local moments of both chains on the AF coupling $|J_2|/J_1$ for a constant $h^z/J_1 = 1.0$, where this phase can be found. As $|J_2|/J_1$ increases from zero, the total magnetization (red curve) smoothly decreases from $M/M_{\text{sat}} = 0.8$ to approximately $M/M_{\text{sat}} = 1/2$ for $|J_2|/J_1 \gtrsim 1.0$, reflecting the occurrence of a one-half magnetization plateau state. The average local moments reveal that this plateau is characterized by a polarization of chain 1 (gray dashed curve), whose magnetization remains nearly constant across the entire field range. In contrast, chain 2 (black curve) undergoes a continuous suppression of its average local moment, nearly vanishing as $|J_2|/J_1 \rightarrow 1.0$. Beyond this point, chain 2 enters a nonmagnetic state,

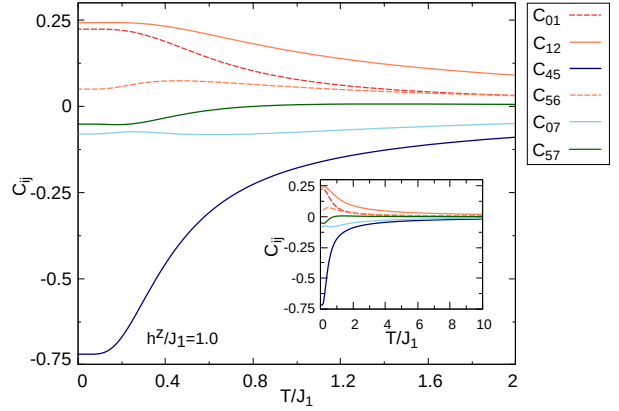


Figure 7: Spin-spin correlations C_{ij} as a function of temperature within the eight-site CMF approach at constant field $h^z/J_1 = 1.0$. Some correlations have been omitted from the figure as they are nearly equivalent to those already shown, e.g., the correlations $C_{01} \approx C_{23}$, $C_{45} \approx C_{67}$, $C_{46} \approx C_{57}$ and the interchain correlations $C_{07} \approx C_{16}$ $\approx C_{25} \approx C_{34}$.

consistent with the formation of a dimer phase, as illustrated schematically in the inset. Therefore, the strength of the AF coupling J_2 drives the system into a coexisting FM-dimerized phase, where chain 1 retains the long-range FM order and chain 2 forms singlet pairs. Our analysis suggests that fine-tuning of J_n allows control over the magnetic nature of the system under an external magnetic field, mainly adjusting the degree of frustration. This mechanism may supply pathways for engineering exotic magnetic phases in other verdazyl-based compounds.

3.2. Finite temperature correlations

The temperature dependence of the spin-spin correlation functions under an applied magnetic field $h^z/J_1 = 1.0$ provides further insight into the stability of the field-induced phases. As shown in Fig. 7, the correlations of chain 1 (C_{01}, C_{12}, C_{23}) reflect its FM polarization along the field direction, remaining close to 0.25 at low temperatures and decaying to zero as the temperature increases. In contrast, the correlations C_{45} and C_{56} in chain 2 exhibit a different behavior at low temperatures, where C_{45} approaches the perfect singlet value of -0.75 , and C_{56} is significantly suppressed, consistent with the emergence of a dimer phase in chain 2. As the temperature increases, these correlations in chain 2 progressively weaken, signaling thermal suppression of the singlet states. In agreement with the previous discussion, the interchain correlations (C_{07}, C_{16}, \dots) and the correlation C_{57} remain negligible throughout the temperature range. These results indicate that, under a range of ap-

plied fields, the system can stabilize a coexisting FM-dimerized phase at low temperatures.

4. Summary and conclusion

We employed the CMF method to investigate the spin-1/2 Heisenberg model on an anisotropic square lattice inspired by the verdazyl-based compound (*o*-MePy-V)PF₆. This model features six distinct FM and AF nearest-neighbor exchange interactions within two AF coupled quantum spin chains: one FM and the other FM-AF. We explored slightly modified combinations of these interactions to investigate the effect of varying degrees of frustration on the magnetic properties of the model. Our discussion focuses on local magnetization patterns, average local moments, and spin–spin correlation functions under magnetic fields.

In the ground state, the local magnetization patterns recover the results obtained for the reference compound, exhibiting a collinear AF order in the transverse plane characterized by a twofold periodic structure [15, 17]. Small variations in the exchange couplings relative to the reference values can also drive a similar AF collinear order at zero field. However, these variations can give rise to a nontrivial magnetic behavior under an applied magnetic field. This becomes evident when the degree of frustration is increased by strengthening the AF character of the FM-AF chain. In the presence of an external field, a nonmagnetic state emerges as a consequence of quantum fluctuations induced by the field in this chain, characterized by the vanishing of both longitudinal and transverse local magnetizations, while the other chain develops a FM order. As a result, a one-half magnetization plateau can be found in a range of applied fields. This means that small changes in the coupling parameters of the reference system can change the magnetization profile from a plateau-like regime to a well-defined magnetization plateau. More importantly, the spin–spin correlation functions reveal the formation of spin-singlet pairs in the one-half magnetization plateau regime. The FM-AF chain exhibits both the absence of local magnetic order and the presence of uncorrelated spin-singlet pairs, indicating a dimerized phase. Therefore, the ground state of the system with an enhanced degree of frustration can include a coexisting FM-dimerized phase induced by an external field. This coexistence can also persist for low temperatures.

To conclude, the interplay between frustration and field-induced quantum fluctuations can drive the stabilization of exotic behaviors, such as the FM-dimerized phase. Remarkably, the degree of frustration required to obtain the FM-dimerized phase in such systems can be

accessed by tuning the spin anisotropies of the reference compound [17], or by adjusting the exchange parameters, as demonstrated in the present work. These findings not only deepen our understanding of frustration-driven quantum phenomena but also offer valuable guidance for engineering novel magnetic phases in verdazyl-based compounds and other strongly correlated quantum magnets.

Acknowledgment

This work was supported by the Brazilian agencies Conselho Nacional de Desenvolvimento Científico e Tecnológico (CNPq), Grant Nos. 165330/2023-6 and 309652/2023-5, and Coordenação de Aperfeiçoamento de Pessoal de Nível Superior (Capes). FMZ and LMR also acknowledge support from the Fundação de Apoio ao Desenvolvimento do Ensino, Ciência e Tecnologia do Estado de Mato Grosso do Sul (Fundect).

Data availability

The data that support the findings of this study are available from the corresponding author upon reasonable request.

References

- [1] L. Savary, L. Balents, Quantum spin liquids: a review, *Reports on Progress in Physics* 80 (2016) 016502. URL: <https://dx.doi.org/10.1088/0034-4885/80/1/016502>.
- [2] Y. Zhou, K. Kanoda, T.-K. Ng, Quantum spin liquid states, *Rev. Mod. Phys.* 89 (2017) 025003. URL: <https://link.aps.org/doi/10.1103/RevModPhys.89.025003>.
- [3] H.-C. Jiang, H. Yao, L. Balents, Spin liquid ground state of the spin- $\frac{1}{2}$ square J_1 - J_2 heisenberg model, *Phys. Rev. B* 86 (2012) 024424. URL: <https://link.aps.org/doi/10.1103/PhysRevB.86.024424>.
- [4] A. Metavitsiadis, D. Sellmann, S. Eggert, Spin-liquid versus dimer phases in an anisotropic J_1 - J_2 frustrated square antiferromagnet, *Phys. Rev. B* 89 (2014) 241104. URL: <https://link.aps.org/doi/10.1103/PhysRevB.89.241104>.

[5] W.-Y. Liu, S.-S. Gong, Y.-B. Li, D. Poilblanc, W.-Q. Chen, Z.-C. Gu, Gapless quantum spin liquid and global phase diagram of the spin-1/2 $J_1 - J_2$ square antiferromagnetic heisenberg model, *Science Bulletin* 67 (2022) 1034–1041. URL: <https://www.sciencedirect.com/science/article/pii/S2095927322001001>. doi:<https://doi.org/10.1016/j.scib.2022.03.010>.

[6] N. Xi, H. Chen, Z. Y. Xie, R. Yu, Plaquette valence bond solid to antiferromagnet transition and deconfined quantum critical point of the shastry-sutherland model, *Phys. Rev. B* 107 (2023) L220408. URL: <https://link.aps.org/doi/10.1103/PhysRevB.107.L220408>. doi:[10.1103/PhysRevB.107.L220408](https://doi.org/10.1103/PhysRevB.107.L220408).

[7] Z. H. Li, X. T. Han, C. Dong, H. W. Wang, Z. Z. He, R. Chen, W. X. Liu, C. L. Lu, Y. Kohama, M. Tokunaga, K. Kindo, Z. W. Ouyang, J. F. Wang, M. Yang, Dimerization-enhanced exotic magnetization plateau and magnetoelectric phase diagrams in skew-chain $\text{Co}_2\text{V}_2\text{O}_7$, *Phys. Rev. B* 109 (2024) 094432. URL: <https://link.aps.org/doi/10.1103/PhysRevB.109.094432>. doi:[10.1103/PhysRevB.109.094432](https://doi.org/10.1103/PhysRevB.109.094432).

[8] N. Laflorencie, D. J. Luitz, F. Alet, Spin-wave approach for entanglement entropies of the $J_1 - J_2$ heisenberg antiferromagnet on the square lattice, *Phys. Rev. B* 92 (2015) 115126. URL: <https://link.aps.org/doi/10.1103/PhysRevB.92.115126>. doi:[10.1103/PhysRevB.92.115126](https://doi.org/10.1103/PhysRevB.92.115126).

[9] H. F. Song, N. Laflorencie, S. Rachel, K. Le Hur, Entanglement entropy of the two-dimensional heisenberg antiferromagnet, *Phys. Rev. B* 83 (2011) 224410. URL: <https://link.aps.org/doi/10.1103/PhysRevB.83.224410>. doi:[10.1103/PhysRevB.83.224410](https://doi.org/10.1103/PhysRevB.83.224410).

[10] J. Yang, A. W. Sandvik, L. Wang, Quantum criticality and spin liquid phase in the shastry-sutherland model, *Phys. Rev. B* 105 (2022) L060409. URL: <https://link.aps.org/doi/10.1103/PhysRevB.105.L060409>. doi:[10.1103/PhysRevB.105.L060409](https://doi.org/10.1103/PhysRevB.105.L060409).

[11] T. T. Tran, C. A. Pocs, Y. Zhang, M. J. Winiarski, J. Sun, M. Lee, T. M. McQueen, Spinon excitations in the quasi-one-dimensional $s = \frac{1}{2}$ chain compound $\text{Cs}_4\text{CuSb}_2\text{Cl}_{12}$, *Phys. Rev. B* 101 (2020) 235107. URL: <https://link.aps.org/doi/10.1103/PhysRevB.101.235107>. doi:[10.1103/PhysRevB.101.235107](https://doi.org/10.1103/PhysRevB.101.235107).

[12] H. Shao, Y. Q. Qin, S. Capponi, S. Chesi, Z. Y. Meng, A. W. Sandvik, Nearly deconfined spinon excitations in the square-lattice spin-1/2 heisenberg antiferromagnet, *Phys. Rev. X* 7 (2017) 041072. URL: <https://link.aps.org/doi/10.1103/PhysRevX.7.041072>. doi:[10.1103/PhysRevX.7.041072](https://doi.org/10.1103/PhysRevX.7.041072).

[13] A. Honecker, F. Mila, B. Normand, Multi-triplet bound states and finite-temperature dynamics in highly frustrated quantum spin ladders, *Phys. Rev. B* 94 (2016) 094402. URL: <https://link.aps.org/doi/10.1103/PhysRevB.94.094402>. doi:[10.1103/PhysRevB.94.094402](https://doi.org/10.1103/PhysRevB.94.094402).

[14] M. Udono, M. Sato, Triplons, triplon pairs, and dynamical symmetries in laser-driven shastry-sutherland magnets, *Phys. Rev. B* 110 (2024) L201112. URL: <https://link.aps.org/doi/10.1103/PhysRevB.110.L201112>. doi:[10.1103/PhysRevB.110.L201112](https://doi.org/10.1103/PhysRevB.110.L201112).

[15] H. Yamaguchi, Y. Sasaki, T. Okubo, M. Yoshida, T. Kida, M. Hagiwara, Y. Kono, S. Kittaka, T. Sakakibara, M. Takigawa, Y. Iwasaki, Y. Hosokoshi, Field-enhanced quantum fluctuation in an $s = \frac{1}{2}$ frustrated square lattice, *Phys. Rev. B* 98 (2018) 094402. URL: <https://link.aps.org/doi/10.1103/PhysRevB.98.094402>. doi:[10.1103/PhysRevB.98.094402](https://doi.org/10.1103/PhysRevB.98.094402).

[16] H. Yamaguchi, N. Uemoto, T. Okubo, Y. Kono, S. Kittaka, T. Sakakibara, T. Yajima, S. Shimono, Y. Iwasaki, Y. Hosokoshi, Gapped ground state in a spin- $\frac{1}{2}$ frustrated square lattice, *Phys. Rev. B* 104 (2021) L060411. URL: <https://link.aps.org/doi/10.1103/PhysRevB.104.L060411>. doi:[10.1103/PhysRevB.104.L060411](https://doi.org/10.1103/PhysRevB.104.L060411).

[17] L. M. Ramos, F. M. Zimmer, M. Schmidt, Interplay of frustration and quantum fluctuations in a spin-1/2 anisotropic square lattice, *Phys. Rev. B* 112 (2025) 014402. URL: <https://link.aps.org/doi/10.1103/svsc-bvjx>. doi:[10.1103/svsc-bvjx](https://doi.org/10.1103/svsc-bvjx).

[18] R. Moessner, A. P. Ramirez, Geometrical frustration, *Physics Today* 59 (2006) 24–29. URL: <https://doi.org/10.1063/1.2186278>. doi:[10.1063/1.2186278](https://doi.org/10.1063/1.2186278).

[19] K. Wang, X.-J. Liu, L.-M. Tu, J.-J. Zhang, V. N. Gladilin, J.-Y. Ge, Experimental realization of antiferromagnetic ising ground state on the triangular lattice, *Phys. Rev. B* 111 (2025) 224418. URL: <https://link.aps.org/doi/10.1103/PhysRevB.111.224418>. doi:10.1103/PhysRevB.111.224418.

[20] J. A. Mydosh, Spin glasses: redux: an updated experimental/materials survey, *Reports on Progress in Physics* 78 (2015) 052501. URL: <https://dx.doi.org/10.1088/0034-4885/78/5/052501>. doi:10.1088/0034-4885/78/5/052501.

[21] E. C. Andrade, J. A. Hoyos, S. Rachel, M. Vojta, Cluster-glass phase in pyrochlore xy antiferromagnets with quenched disorder, *Phys. Rev. Lett.* 120 (2018) 097204. URL: <https://link.aps.org/doi/10.1103/PhysRevLett.120.097204>. doi:10.1103/PhysRevLett.120.097204.

[22] M. Schmidt, F. M. Zimmer, S. G. Magalhaes, Spin liquid and infinitesimal-disorder-driven cluster spin glass in the kagome lattice, *Journal of Physics: Condensed Matter* 29 (2017) 165801. URL: <https://dx.doi.org/10.1088/1361-648X/aa6060>. doi:10.1088/1361-648X/aa6060.

[23] F. M. Zimmer, C. F. Silva, S. G. Magalhaes, C. Lacroix, Interplay between spin-glass clusters and geometrical frustration, *Phys. Rev. E* 89 (2014) 022120. URL: <https://link.aps.org/doi/10.1103/PhysRevE.89.022120>. doi:10.1103/PhysRevE.89.022120.

[24] S.-W. Li, F.-J. Jiang, A comprehensive study of the phase transitions of the frustrated j_1 - j_2 ising model on the square lattice, *Progress of Theoretical and Experimental Physics* 2024 (2024) 053A06. URL: <https://doi.org/10.1093/ptep/ptae061>. doi:10.1093/ptep/ptae061.

[25] H. Yamaguchi, Y. Iwasaki, Y. Kono, T. Okubo, S. Miyamoto, Y. Hosokoshi, A. Matsuo, T. Sakakibara, T. Kida, M. Hagiwara, Quantum critical phenomena in a spin- $\frac{1}{2}$ frustrated square lattice with spatial anisotropy, *Phys. Rev. B* 103 (2021) L220407. URL: <https://link.aps.org/doi/10.1103/PhysRevB.103.L220407>. doi:10.1103/PhysRevB.103.L220407.

[26] G.-H. Liu, H.-L. Wang, G.-S. Tian, Existence of dimerized phases in frustrated spin ladder models, *Phys. Rev. B* 77 (2008) 214418. URL: <https://link.aps.org/doi/10.1103/PhysRevB.77.214418>. doi:10.1103/PhysRevB.77.214418.

[27] S. Wessel, B. Normand, F. Mila, A. Honecker, Efficient Quantum Monte Carlo simulations of highly frustrated magnets: the frustrated spin-1/2 ladder, *SciPost Phys.* 3 (2017) 005. URL: <https://scipost.org/10.21468/SciPostPhys.3.1.005>. doi:10.21468/SciPostPhys.3.1.005.

[28] D. S. Almeida, A. S. Bibiano-Filho, W. M. da Silva, R. R. Montenegro-Filho, Mixed-spin heisenberg ladders in a magnetic field, *Phys. Rev. E* 111 (2025) 014149. URL: <https://link.aps.org/doi/10.1103/PhysRevE.111.014149>. doi:10.1103/PhysRevE.111.014149.

[29] H. Saito, C. Hotta, Phase diagram of the quantum spin- $\frac{1}{2}$ heisenberg- Γ model on a frustrated zigzag chain, *Phys. Rev. B* 110 (2024) 024409. URL: <https://link.aps.org/doi/10.1103/PhysRevB.110.024409>. doi:10.1103/PhysRevB.110.024409.

[30] D. Yamamoto, G. Marmorini, I. Danshita, Quantum phase diagram of the triangular-lattice xxz model in a magnetic field, *Phys. Rev. Lett.* 112 (2014) 127203. URL: <https://link.aps.org/doi/10.1103/PhysRevLett.112.127203>. doi:10.1103/PhysRevLett.112.127203.

[31] D. Yamamoto, G. Marmorini, I. Danshita, Microscopic model calculations for the magnetization process of layered triangular-lattice quantum antiferromagnets, *Phys. Rev. Lett.* 114 (2015) 027201. URL: <https://link.aps.org/doi/10.1103/PhysRevLett.114.027201>. doi:10.1103/PhysRevLett.114.027201.

[32] D. Yamamoto, H. Ueda, I. Danshita, G. Marmorini, T. Momoi, T. Shimokawa, Exact diagonalization and cluster mean-field study of triangular-lattice xxz antiferromagnets near saturation, *Phys. Rev. B* 96 (2017) 014431. URL: <https://link.aps.org/doi/10.1103/PhysRevB.96.014431>. doi:10.1103/PhysRevB.96.014431.

[33] A. Singhania, S. Kumar, Cluster mean-field study of the Heisenberg model for CuInVO_5 , *Phys. Rev. B* 98 (2018) 104429. URL: <https://link.aps.org/doi/10.1103/PhysRevB.98.104429>.

org/doi/10.1103/PhysRevB.98.104429.
doi:10.1103/PhysRevB.98.104429.

- [34] N. Kellermann, M. Schmidt, F. M. Zimmer, Quantum ising model on the frustrated square lattice, *Phys. Rev. E* 99 (2019) 012134. URL: <https://link.aps.org/doi/10.1103/PhysRevE.99.012134>. doi:10.1103/PhysRevE.99.012134.
- [35] M. Pikulski, T. Shiroka, F. Casola, A. P. Reyes, P. L. Kuhns, S. Wang, H.-R. Ott, J. Mesot, Two coupled chains are simpler than one: field-induced chirality in a frustrated spin ladder, *Scientific Reports* 10 (2020). URL: <https://doi.org/10.1038/s41598-020-72215-z>. doi:10.1038/s41598-020-72215-z.
- [36] K. Karl'ová, J. Strečka, M. L. Lyra, Breakdown of intermediate one-half magnetization plateau of spin-1/2 ising-heisenberg and heisenberg branched chains at triple and kosterlitz-thouless critical points, *Phys. Rev. E* 100 (2019) 042127. URL: <https://link.aps.org/doi/10.1103/PhysRevE.100.042127>. doi:10.1103/PhysRevE.100.042127.
- [37] R. R. Montenegro-Filho, E. J. P. Silva-Júnior, M. D. Coutinho-Filho, Ground-state phase diagram and thermodynamics of coupled trimer chains, *Phys. Rev. B* 105 (2022) 134423. URL: <https://link.aps.org/doi/10.1103/PhysRevB.105.134423>. doi:10.1103/PhysRevB.105.134423.
- [38] T. Picot, M. Ziegler, R. Orús, D. Poilblanc, Spin- s kagome quantum antiferromagnets in a field with tensor networks, *Phys. Rev. B* 93 (2016) 060407. URL: <https://link.aps.org/doi/10.1103/PhysRevB.93.060407>. doi:10.1103/PhysRevB.93.060407.